

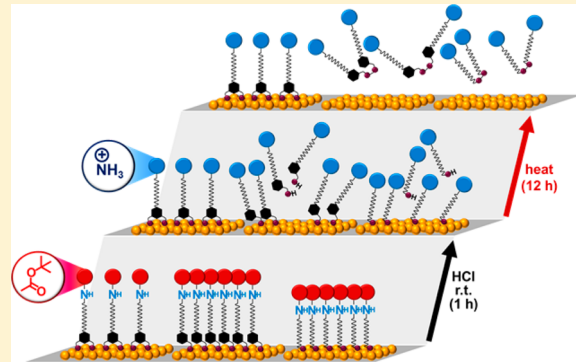
## Boc-Protected $\omega$ -Amino Alkanedithiols Provide Chemically and Thermally Stable Amine-Terminated Monolayers on Gold

Han Ju Lee, Andrew C. Jamison, and T. Randall Lee\*

Department of Chemistry and the Texas Center for Superconductivity, University of Houston, 4800 Calhoun Road, Houston, Texas 77204-5003, United States

Supporting Information

**ABSTRACT:** Four custom-designed bidentate adsorbates having either ammonium or Boc-protected amino termini and either methanethiol or ethanethioate headgroups were prepared for the purpose of generating amine-terminated self-assembled monolayers (SAMs) on evaporated gold surfaces. These adsorbates utilize a phenyl-based framework to connect the headgroups to a single hexadecyloxy chain, extending the amino functionality away from the surface of gold, providing two regions within the adsorbate structure where intermolecular interactions contribute to the stability of the fully formed thin film. The structural features of the resulting SAMs were characterized by ellipsometry, X-ray photoelectron spectroscopy, and polarization modulation infrared reflection–absorption spectroscopy. The collected data were compared to those of eight additional SAMs formed from analogous monodentate alkanethiols and alkanethioacetates having either a similar aromatic framework or a simple alkyl chain connecting the headgroup to the tailgroup. The analysis of the data obtained for the full set of SAMs revealed that both the tailgroup and headgroup influenced the formation of a well-packed monolayer, with the Boc-protected amine-terminated alkanethiols producing films with superior surface bonding and adsorbate packing as compared to those formed with ammonium tailgroups or alkanethioacetate headgroups. A comparison of the structural differences before and after deprotection of the Boc-protected amine-terminated thiolate SAMs revealed that the bidentate adsorbate was the most resistant to desorption during the Boc-deprotection procedure. Furthermore, solution-phase thermal desorption tests performed to evaluate the thermal stability of the Boc-deprotected amine-terminated alkanethiolate films provided further evidence of the enhanced stability associated with SAMs formed from these bidentate adsorbates.



### INTRODUCTION

Amine-functionalized surfaces have been intensively pursued to develop interfacial platforms for creating new electronic devices,<sup>1–3</sup> sensors,<sup>4–7</sup> and biomaterials<sup>8,9</sup> due to their versatility in forming chemical bonds (e.g., covalent, ionic, and hydrogen bonds). For example, Bao and coworkers prepared single-walled nanotube (SWNT) arrays for carbon nanotube field-effect transistors that were immobilized on amine-terminated silicon oxide surfaces via electrostatic interactions with carboxylate groups on SWNTs.<sup>1</sup> Bunimovich et al. demonstrated the importance of the specific procedure used for the development of DNA sensing properties for amine-functionalized silicon nanowires (SiNWs), preparing samples from either hydrogen-terminated surfaces or silicon surfaces where a native oxide coating was present.<sup>4</sup> The electrostatic interaction between the amine termini and the DNA strands, absent an underlying oxidized silica surface, played an important role in improving the sensitivity of their sensor. Amine-terminated gold substrates have also been prepared for the surface attachment of DNA.<sup>6</sup> In a report by Brockman et al., DNA was covalently bound to an amine-terminated surface formed from 11-mercaptopoundecylamine via

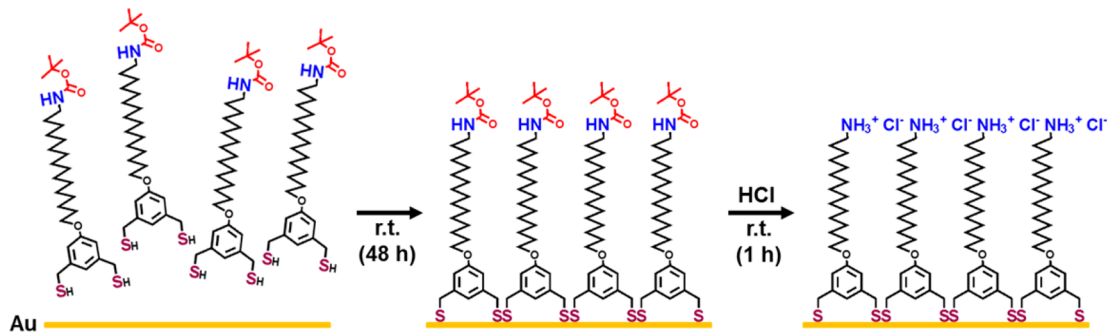
a sulfosuccinimidyl 4-(*N*-maleimidomethyl)-cyclohexane-1-carboxylate (SSMCC) linker.

Self-assembled monolayers (SAMs) have proven to be a reliable technology for the surface modification of metals and various oxide surfaces and have played a key role in the development of amine-functionalized surfaces. Amine-terminated alkylsilanes have been widely used for the amine functionalization of surfaces such as silicon oxide<sup>1,2,4,5</sup> and indium tin oxide (ITO)<sup>10</sup> via their strong Si–O covalent linkages. However, these alkylsilanes are unstable compounds themselves, which can contribute to difficulties in the formation of well-ordered films.<sup>11</sup> This problem is exemplified by the short-lived pentacoordinate complexes that can be generated by a self-catalyzed reaction of such amine-terminated alkylsilanes and by their propensity to polymerize in the presence of water.<sup>11,12</sup> Therefore, a dry environment is usually required when such alkylsilane compounds are used.

Received: November 12, 2014

Revised: January 24, 2015

Published: January 28, 2015

Scheme 1. Formation of Amine-Terminated SAMs by Adsorption and Deprotection of Boc-Protected  $\omega$ -Amino Alkanedithiols

A slightly different problem exists for incorporating an amino group within the same molecular structure as a thiol; namely, the basicity of the amine creates an environment that is conducive to oxidizing the thiol under ambient conditions. To functionalize the surfaces of coinage metals such as gold, silver, and copper, ammonium-terminated alkanethiols have been prepared.<sup>13</sup> These thiols are less sensitive to moisture than amine-terminated alkylsilanes, but other problems are associated with their use. First, ammonium-terminated alkanethiols easily form double layers on substrates due to hydrogen bonding or electrostatic interactions between amine or ammonium terminal groups in freshly formed SAMs in contact with amine- or ammonium-terminated adsorbates in bulk solution.<sup>14,15</sup> Second, these same interactions between terminal groups also interfere with the formation of well-ordered monolayers.<sup>15</sup> Third, oxidized sulfur species have been frequently detected in the SAMs generated from ammonium-terminated alkanethiols, unlike SAMs derived from normal alkanethiols.<sup>15–17</sup> Fourth, terminal amino groups form carbamate salts when exposed to atmospheric carbon dioxide.<sup>6,18</sup> Despite these concerns, amine-functionalized surfaces continue to be pursued for a variety of research objectives.

Recently, several research groups reported nano- and micropatterned amine-terminated surfaces formed from various types of protected-amine surfactants.<sup>19–23</sup> Fréchet and co-workers prepared  $\alpha,\alpha$ -dimethyl-3,5-dimethoxybenzyloxycarbonyl (DDZ)- and benzoquinone-protected amine-terminated alkylsilanes for use as monolayer precursors.<sup>19,20</sup> After preparing SAMs on silicon oxide surfaces with their custom-designed adsorbates, the authors generated nanosized patterns using AFM lithography to initiate the deprotection of the amino groups. Shestopalov et al. used *tert*-butoxycarbonyl (Boc)-protected amine-terminated alkenes to produce SAMs on H-terminated silicon via a UV-light-initiated surface reaction.<sup>21</sup> However, the micrometer-sized patterns were generated by a microcontact printing ( $\mu$ CP) technique instead of AFM lithography. The same research team also demonstrated the production of patterned amine-terminated SAMs on gold surfaces using 9-fluorenylmethoxycarbonyl- (Fmoc-) and Boc-protected alkanethiols.<sup>22,23</sup> To confirm the successful deprotection of the terminal amino groups, the authors evaluated the carbon-to-gold (C/Au) ratios obtained from X-ray photoelectron spectroscopy (XPS) before and after patterning (deprotection). Interestingly, the C/Si ratio for the study involving the deprotection of SAMs formed on silicon oxide decreased  $\sim$ 13% from the initial ratio for the Boc-protected amine-functionalized monolayers, but for the Boc- and Fmoc-amine-functionalized gold systems, the decreases in

the C/Au ratios were 31 and 52%, respectively, which correspond to a larger decrease in carbon content than that anticipated for just the deprotection. These results can be rationalized by considering the nature of the bonding between the adsorbates/precursors and substrates. The thermal stability and chemical resistance of the bonds for thiolate SAMs on gold are weaker than those of the bonds between carbon and silicon in SAMs generated from alkene precursors. Therefore, partial desorption of the adsorbates from gold surfaces can occur during the Boc- and Fmoc-deprotection procedures. This loss of adsorbate content for these SAMs diminishes the stability of the remaining film, increasing the likelihood that any molecules bound to the exposed amino groups will detach from the surface in tandem with an oxidized thiolate adsorbate. In the present study, we wish to address the issue of amine-terminated SAM stability by using custom-designed multidentate adsorbates such as that shown in Scheme 1.

Over the past 15 years, our research group has been exploring the efficacy of the chelate effect afforded by multidentate alkanethiols in enhancing the stability of SAMs on gold surfaces.<sup>24–31</sup> Recently, we demonstrated the remarkable stability of carboxylic acid-terminated SAMs generated from custom-designed aromatic bidentate thiols.<sup>31</sup> These adsorbates were found to be stable on both flat and curved gold surfaces in polar and nonpolar solvents at 90 °C. The film-formation challenges and functional advantages of these carboxylic acid tailgroups share similarities with those of the presently targeted amine-terminated SAMs. Bruno and coworkers have also demonstrated the enhanced thermal stability of SAMs generated from bidentate adsorbates possessing an aromatic moiety.<sup>32</sup> Their study revealed that aromatic dithiols were more thermally stable than aromatic monothiols using a thermal annealing test of aromatic thiol-functionalized gold nanoparticles. Prior studies showing that alkanethioacetates can directly form SAMs without being converted to alkanethiols<sup>33,34</sup> are relevant to the current investigation because we felt that the use of thioacetate groups would inhibit bilayer formation during the self-assembly of amine-terminated alkanethiols on gold by eliminating interactions between the basic amino groups and the acidic thiol groups.

To determine the adsorbate structural parameters that would provide optimal access to stable ammonium- or amine-terminated alkanethiolate films, we designed and synthesized four classes of adsorbates consisting of ammonium or Boc-protected amino tailgroups coupled with thiol or thioacetate headgroups. The bidentate adsorbates (dithiol, DT; or dithioacetate, DTA) analyzed in this report contain an aromatic ring (phenyl, P) as part of the headgroup with an alkyl chain

(hexadecyl, H) connecting the tailgroup (ammonium, A; or Boc-protected amine, Boc-A) to the ring, as shown in Figure 1.

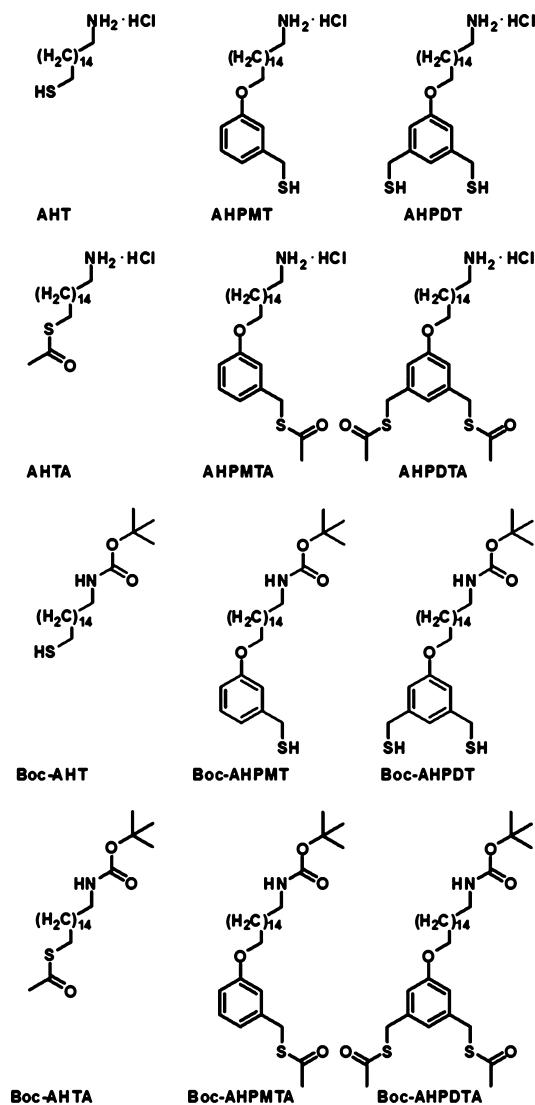


**Figure 1.** Structures of the ammonium- and Boc-protected amine-terminated adsorbates.

These compounds are an ammonium-terminated alkanethiol [(5-(16-aminohexadecyloxy)-1,3-phenylene)dimethanethiol hydrochloride (**AHPDT**)], an ammonium-terminated alkane-thioacetate [*S,S'*-(5-(16-aminohexa-decyloxy)-1,3-phenylene)-bis(methylene) diethanethioate hydrochloride (**AHPDTA**)], a Boc-protected amine-terminated alkanethiol [*tert*-butyl 16-(3,5-bis(mercaptomethyl)phenoxy)hexadecylcarbamate (**Boc-AHPDT**)], and a Boc-protected amine-terminated alkanethioacetate [*S,S'*-(5-(*tert*-butoxycarbonylamo)hexadecyloxy)-1,3-phenylene)bis(methylene) diethanethioate (**Boc-AHPDTA**)]. To provide a more complete analysis of the effectiveness of these new adsorbates, analogous monodentate adsorbates (monothiol, MT) and simpler functionalized alkanethiols (thiol, T) were prepared (Figure 1). The monothiol compounds incorporating an aromatic moiety are (3-(16-aminohexadecyloxy)phenyl)methanethiol hydrochloride (**AHPMT**), S-3-(16-aminohexadecyloxy)benzyl ethanethioate hydrochloride (**AHPMTA**), *tert*-butyl 16-(3-(mercaptomethyl)phenoxy)hexadecylcarbamate (**Boc-AHPMT**), and S-3-(16-

(*tert*-butoxycarbonylamo)hexadecyloxy)benzyl ethanethioate (**Boc-AHPMTA**). The analogous simple alkanethiol adsorbates are 16-aminohexadecane-1-thiol hydrochloride (**AHT**), S-16-aminohexadecyl ethanethioate hydrochloride (**AHTA**), *tert*-butyl 16-mercaptophexadecyl-carbamate (**Boc-AHT**), and S-16-(*tert*-butoxycarbonylamo)hexadecyl ethanethioate (**Boc-AHTA**).

Herein, we explore amine-terminated SAMs prepared from the set of 12 adsorbates displayed in Figure 1 and from octadecanethiol (**C18SH**), which serves as a reference standard for thiolate SAMs on evaporated “flat” gold. Structural analysis of the SAMs was conducted by ellipsometry, XPS, and polarization modulation infrared reflection-absorption spectroscopy (PM-IRRAS). Structural differences for the Boc-protected amine-terminated SAMs before and after deprotection were evaluated using contact angle measurements coupled with ellipsometry, XPS, and PM-IRRAS. Furthermore, a thermal stability study of the Boc-deprotected amine-terminated thiolate SAMs was conducted to evaluate their potential as fundamental thin-film components for new material constructs and device architectures.

## EXPERIMENTAL SECTION

Complete details regarding the materials, procedures, and instrumentation used to conduct the research reported here are provided in the Supporting Information, including <sup>1</sup>H and <sup>13</sup>C NMR spectra for all new thioadsorbates (Figures S1–S16).

## RESULTS AND DISCUSSION

**Characterization of Ammonium- and Boc-Protected Amine-Terminated SAMs on Evaporated Gold Surfaces.** Evaporated gold slides were immersed in 3 mM solutions for each of the thiols and thioacetates for 48 h at room temperature. Deposition solutions were prepared using both ethanol (EtOH) and tetrahydrofuran (THF) as the solvent medium. The resultant thin films were characterized by ellipsometry, XPS, and PM-IRRAS.

**Formation of SAMs on Gold Surfaces.** To verify that SAMs were produced with complete or nearly complete bonding between the sulfur moieties of the adsorbates and the gold substrates, without the formation of multilayers, we conducted analyses by XPS and ellipsometry. The data collected by XPS for this series of SAMs reveal the nature of the Au–S bonds through deconvolution of the binding energy (BE) peaks in the S 2p region of the XPS spectra.<sup>35</sup> The S 2p<sub>3/2</sub> and S 2p<sub>1/2</sub> peaks of bound thiolate appear at ~162.0 and ~163.2 eV, respectively, with a 2:1 peak area ratio. Peaks in the range of 164–166 eV would indicate the presence of unbound thiol or disulfides, and peaks at ~169 eV would indicate the presence of oxidized sulfur species. Three noteworthy observations can be made with regard to the XPS S 2p spectral data in Figure 2: (1) the S 2p<sub>3/2</sub> peaks for unbound thiol (~164 eV) are larger than those for bound thiolates (~162.0 eV) in the XPS spectra for most of the SAMs generated from ammonium-terminated alkanethiols and thioacetates (Figure 2, plots A1, A2, B1, and B2) and from Boc-protected amine-terminated alkanethioacetates (Figure 2, plots A4 and B4); (2) oxidized sulfur species were detected in the XPS spectra for SAMs generated from ammonium-terminated alkanedithiols and alkanedithioacetates (Figure 2, plots A1, A2, B1, and B2), results that align with those for amine-terminated SAMs generated from ammonium-terminated alkanethiols reported in the literature;<sup>15–17</sup> and (3) the XPS spectra for SAMs generated from the Boc-protected

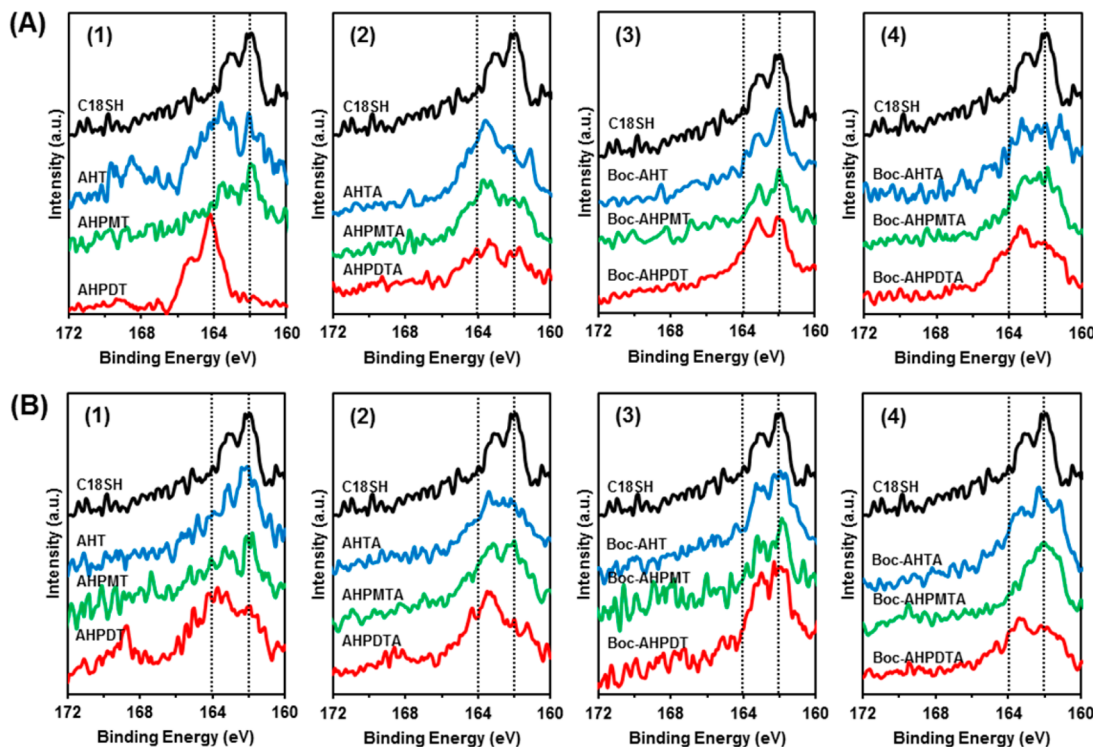


**Figure 2.** XPS spectra of the S 2p region of the SAMs derived from (1) the ammonium-terminated alkanethiols (**AHT**, **AHPMT**, and **AHPDT**), (2) the ammonium-terminated alkanethioacetates (**AHTA**, **AHPMTA**, and **AHPDTA**), (3) the Boc-protected amine-terminated alkanethiols (**Boc-AHT**, **Boc-AHPMT**, and **Boc-AHPDT**), and (4) the Boc-protected amine-terminated alkanethioacetates (**Boc-AHTA**, **Boc-AHPMTA**, and **Boc-AHPDTA**) in (A) ethanol and (B) THF. The corresponding XPS spectrum of the S 2p region of the film generated from **C18SH** in ethanol is shown for reference. Dashed lines provide a means of identifying peaks associated with bound thiolate (~162 eV) and unbound thiol or disulfides (~164 eV).

amine-terminated alkanethiols (Figure 2, plots A3 and B3) reveal strong peaks for bound thiol (~162.0–163.2 eV) but show little or no unbound thiol/disulfides (~164–166 eV) or oxidized sulfur species (~169 eV).

For a more quantitative analysis of the XPS data, the percentages of bound thiolate were evaluated by deconvolution of the peaks in the S 2p region of the XPS spectra, as demonstrated in a previous report.<sup>36</sup> The deconvoluted spectra are provided in the Supporting Information (Figures S17 and S18). Table 1 shows that the percentages of bound thiolate for SAMs generated from the Boc-protected amine-terminated alkanethiols in both ethanol and THF were consistently above 85%, but the other SAM systems failed to provide such reliable results.

To determine the effectiveness of these adsorbates for creating fully formed monolayer films, we also measured the film thicknesses using ellipsometry and compared these thickness measurements to those obtained from a study of SAMs formed from similarly structured carboxylic acid-terminated alkanethiols.<sup>31</sup> Table 1 provides useful insight into the influence of the tailgroup on film formation. The ellipsometric thicknesses of SAMs generated from ammonium-terminated alkanethiols (**AHT**, **AHPMT**, **AHPDT**) in both ethanol and THF were greater than expected when compared to the thickness values of films generated from the reference carboxylic acid-terminated adsorbates. This trend is especially apparent with the ellipsometric thickness of the **AHPDT** film prepared in ethanol, which was 3 times thicker (61 Å) than that of the reference system; furthermore, the **AHPDT** film exhibited an unusually low percentage of bound

**Table 1. Bound Thiolate Percentages Calculated from XPS Data and Ellipsometric Film Thicknesses for Self-Assembled Monolayers Developed in Ethanol and Tetrahydrofuran**

adsorbate	percentage of bound thiolate (%) <sup>a</sup>		ellipsometric thickness (Å) <sup>b</sup>		thicknesses from reference data (Å)
	EtOH	THF	EtOH	THF	
<b>C18SH</b>	99		24		23 <sup>31</sup>
<b>AHT</b>	54	77	27	25	21 <sup>c</sup>
<b>AHPMT</b>	65	71	23	34	27 <sup>c</sup>
<b>AHPDT</b>	8	57	61	33	20 <sup>c</sup>
<b>AHTA</b>	58	71	24	15	21 <sup>c</sup>
<b>AHPMTA</b>	62	73	27	18	27 <sup>c</sup>
<b>AHPDTA</b>	55	55	25	23	20 <sup>c</sup>
<b>Boc-AHT</b>	88	92	25	13	26 <sup>d</sup>
<b>Boc-AHPMT</b>	87	86	33	30	32 <sup>d</sup>
<b>Boc-AHPDT</b>	85	88	27	25	25 <sup>d</sup>
<b>Boc-AHTA</b>	78	84	12	11	26 <sup>d</sup>
<b>Boc-AHPMTA</b>	80	90	17	13	32 <sup>d</sup>
<b>Boc-AHPDTA</b>	63	72	20	15	25 <sup>d</sup>

<sup>a</sup>Percentages of bound thiolate were obtained from the deconvolution of the S 2p peaks of the XPS spectra.<sup>36</sup> <sup>b</sup>Values were taken from three different regions on at least two slides for each adsorbate. The reproducibilities of the ellipsometric thicknesses were within  $\pm 2$  Å.

<sup>c</sup>Reference thicknesses were obtained from SAMs formed from carboxylic acid-terminated adsorbates of similar chain length and structure.<sup>31</sup> <sup>d</sup>Reference thicknesses were estimated by adding the size of the Boc protecting group (~5 Å) to reported thicknesses of SAMs formed from carboxylic acid-terminated adsorbates of similar chain length and structure.<sup>31</sup>

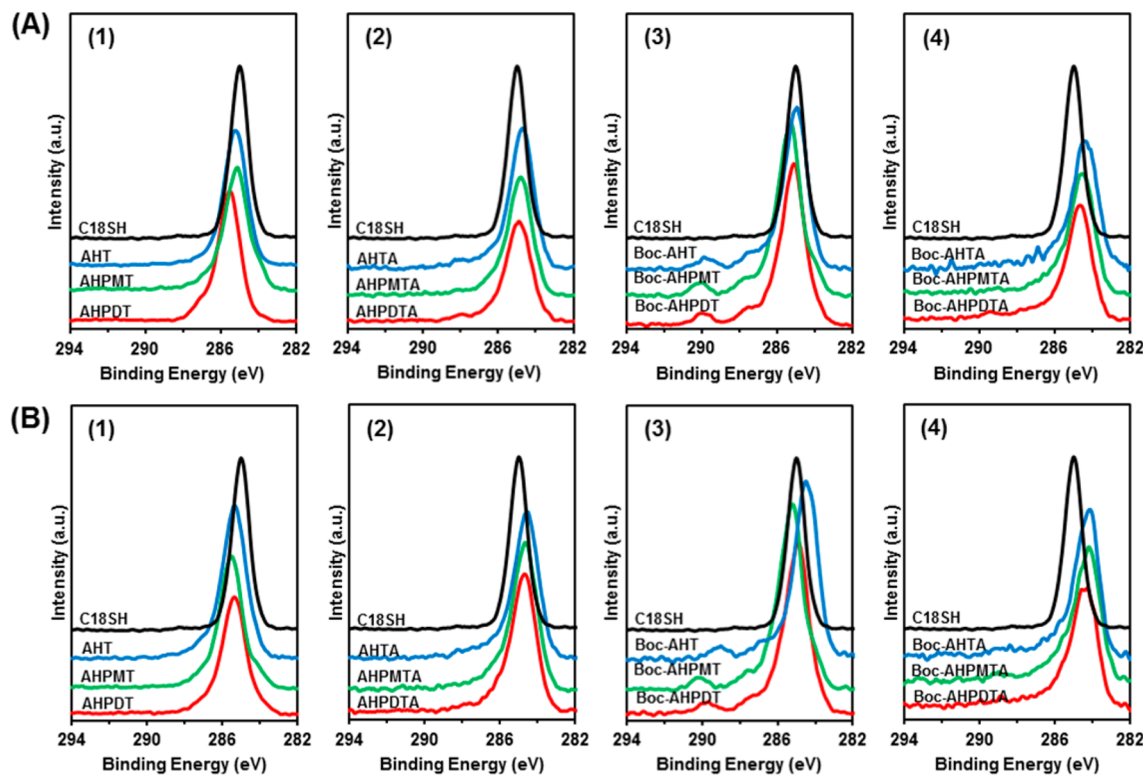


**Figure 3.** XPS spectra of the C 1s region of the SAMs derived from (1) the ammonium-terminated alkanethiols (AHT, AHPMT, and AHPDT), (2) the ammonium-terminated alkanethioacetates (AHTA, AHPMTA, and AHPDTA), (3) the Boc-protected amine-terminated alkanethiols (Boc-AHT, Boc-AHPMT, and Boc-AHPDT), and (4) the Boc-protected amine-terminated alkanethioacetates (Boc-AHTA, Boc-AHPMTA, and Boc-AHPDTA) in (A) ethanol and (B) THF. The corresponding XPS spectrum of the C 1s region of the film generated from C18SH in ethanol is shown for reference.

thiolate (8%). These results are consistent with a model in which **AHPDT** forms multilayer structures via headgroup–tailgroup (thiol–amine) interactions in the SAM. For the ammonium-terminated alkanethioacetate SAMs (**AHTA**, **AHPMTA**, and **AHPDTA**) formed in THF, the thicknesses of the films were smaller than expected for a well-packed SAM, while those formed in EtOH exhibited reasonable thickness values but low bound thiolate percentages. Overall, these data shed doubt on the ability to form well-packed SAMs from thiol-based adsorbates that possess an ammonium terminus.

In contrast, the ellipsometric thicknesses of the films generated from **Boc-AHT**, **Boc-AHPMT**, and **Boc-AHPDT** in ethanol correspond well with the reference values when using our estimated size for the Boc protecting group. The same can be said for the films formed from **Boc-AHPMT** and **Boc-AHPDT** in THF, but the film formed from **Boc-AHT**, the SAM with the highest percentage of bound thiolate (92%), failed to produce a well-packed film. However, all of the SAMs formed from the Boc-protected amine-terminated alkanethioacetates (**Boc-AHTA**, **Boc-AHPMTA**, and **Boc-AHPDTA**) in both ethanol and THF gave thicknesses that were less than the estimated values. We attribute these results, in part, to the bulkiness of the thioacetate headgroup and its impact on film formation.

**SAM Packing Density and Conformational Order.** A comparison of the XPS C 1s spectra for a series of SAMs of similar form and structure can provide insight into the relative packing density of the films as well as the nature of the carbons in the SAMs. The binding energies (BEs) of the carbons in the backbone of alkanethiolate adsorbates are affected by the

packing density of the alkyl chains in the films: positive charges generated by photoelectrons leaving densely packed SAMs are less readily discharged than those in loosely packed SAMs.<sup>27,31,37</sup> This phenomenon creates a shift in the C 1s peak to lower BE for the films with reduced alkyl chain packing, reflecting a change in the distribution of the C 1s BEs. The peak positions for the binding energies of the methylene and aromatic ring carbons of the films generated from **Boc-AHT**, **Boc-AHPMT**, and **Boc-AHPDT** in ethanol were 285.0, 285.2, and 285.0 eV, respectively, and in THF were 284.5, 285.2, and 284.9 eV, respectively (Figure 3, plots A3 and B3). These results can be compared to that of the SAM formed from **C18SH** at 285.0 eV and appear to indicate that the packing densities of the films generated from Boc-protected amine-terminated alkanethiols produce films with alkyl chain packing similar to that of a well-packed normal alkanethiolate SAM. Plots A2, A4, B2, and B4 in Figure 3 show the peaks for the BEs of the carbons composing the backbone of the ammonium- and Boc-protected amine-terminated alkanethioacetate adsorbates, which are all shifted to BEs lower than that of the **C18SH** reference SAM (~0.1–0.9 eV). These results indicate that the alkanethioacetate adsorbates form more loosely packed monolayers on gold substrates. All of the C 1s peaks for the SAMs formed from ammonium-terminated alkanethiols were observed to appear at values greater than 285 eV (Figure 3, plots A1 and B1). We attribute these results to multilayer formation rather than to a well-packed monolayer.<sup>38</sup>

An alternative approach to determining the relative surface order of the adsorbates of a series of SAMs is through a comparison of infrared spectra acquired using surface IR

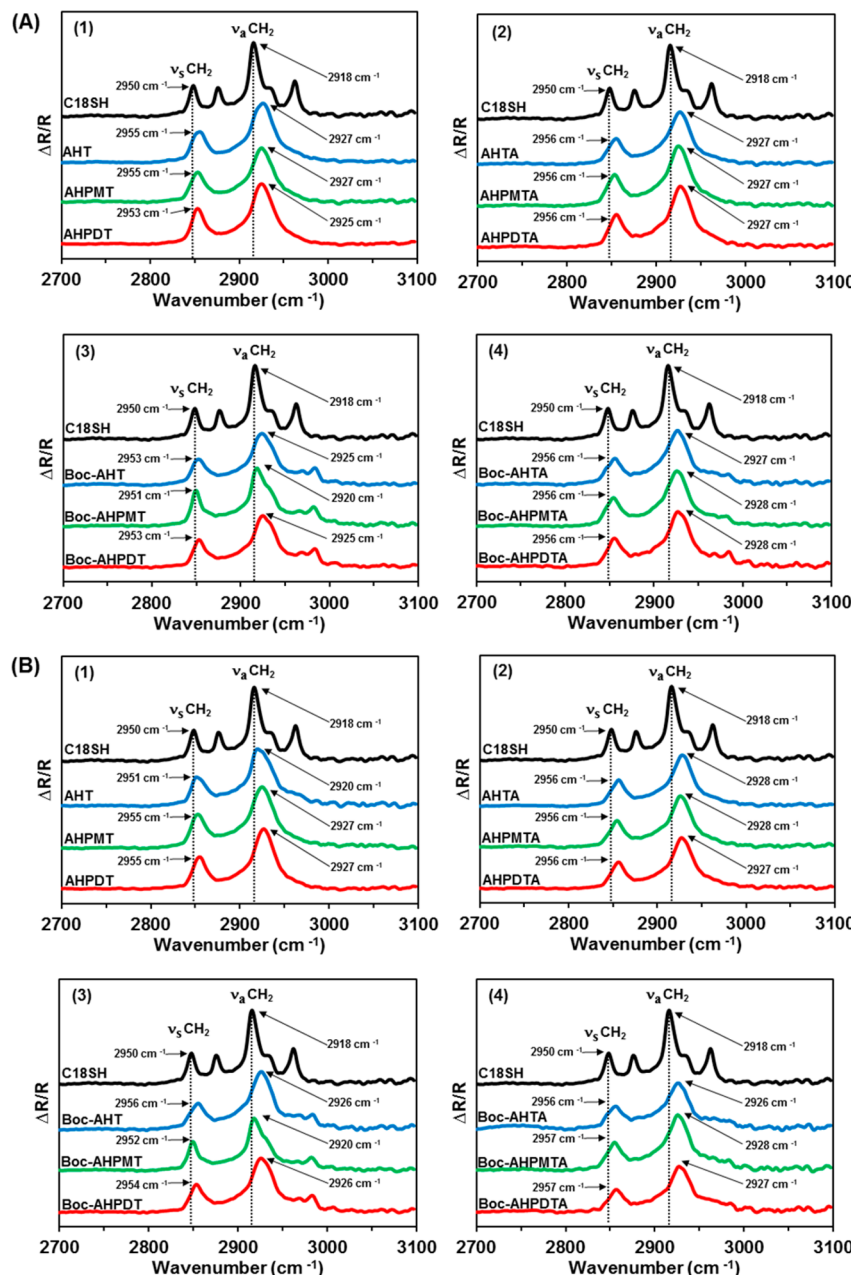


**Figure 4.** PM-IRRAS spectra of the C–H stretching region for the films generated from (1) the ammonium-terminated alkanethiols (AHT, AHPMT, and AHPDT), (2) the ammonium-terminated alkanethioacetates (AHTA, AHPMTA, and AHPDTA), (3) the Boc-protected amine-terminated alkanethiols (Boc-AHT, Boc-AHPMT, and Boc-AHPDT), and (4) the Boc-protected amine-terminated alkanethioacetates (Boc-AHTA, Boc-AHPMTA, and Boc-AHPDTA) in (A) ethanol and (B) THF. The corresponding PM-IRRAS spectrum of the C–H stretching region for the film generated from C18SH in ethanol is shown for reference.

spectroscopy. The peak positions of the methylene antisymmetric and symmetric C–H stretching vibrations ( $\nu_a^{CH_2}$  and  $\nu_s^{CH_2}$ ) obtained using polarization modulation infrared reflection-absorption spectroscopy (PM-IRRAS) can be used to estimate the degree of conformational order of the alkyl chains that form the SAM.<sup>39–41</sup> Plots A2, A4, B2, and B4 in Figure 4 show that the peak positions for  $\nu_a^{CH_2}$  for SAMs generated from ammonium- and Boc-protected amine-terminated alkanethioacetates lie between 2926 and 2928 cm<sup>-1</sup>. According to the interpretation by Porter et al. of IR data collected for long-chain alkanethiol samples in solid and liquid forms, the alkyl chains in these films are primarily liquidlike in character, producing a large number of gauche alignments along

the carbon backbone, as opposed to a lower-energy trans-extended chain alignment typified by the C18SH SAM at ~2918 cm<sup>-1</sup>.<sup>41</sup> Similarly, the alkyl chains for the SAMs generated from the ammonium-terminated alkanethiols were predominantly liquidlike in character, with the exception of AHT at 2920 cm<sup>-1</sup> (Figure 4, plots A1 and B1). The peak positions for  $\nu_a^{CH_2}$  for SAMs generated from Boc-AHT, Boc-AHPMT, and Boc-AHPDT in ethanol are 2925, 2920, and 2925 cm<sup>-1</sup>, respectively, and are slightly better results than the data for the same set of SAMs formed in THF (Figure 4, plots A3 and B3). These results indicate not only that the degree of conformational order of the SAMs derived from Boc-protected amine-terminated alkanethiols is higher than those of SAMs

**Table 2. Ellipsometric Film Thickness and Water Contact Angle Data for the SAMs Generated from Boc-AHT, Boc-AHPMT, and Boc-AHPDT, before and after Deprotection**

	before deprotection (Boc-)			after deprotection (D-)			difference = after – before		
	AHT	AHPMT	AHPDT	AHT	AHPMT	AHPDT	AHT	AHPMT	AHPDT
film thickness <sup>a</sup>	25 Å	33 Å	27 Å	14 Å	19 Å	23 Å	-11 Å	-14 Å	-4 Å
water contact angle	$\theta_a$	90°	99°	90°	76°	72°	<sup>b</sup>	-24°	-27°
	$\theta_r$	66°	79°	69°	45°	43°	<sup>b</sup>	-21°	-36°
	$\Delta$	24°	20°	21°	33°	29°	<sup>b</sup>	+9°	+9°

<sup>a</sup>The reproducibilities of the ellipsometric thicknesses were within  $\pm 2$  Å. <sup>b</sup>Contact angles for water on amine-terminated SAMs generated from Boc-AHPDT were not measurable after deprotection because the surfaces were completely wet by water.

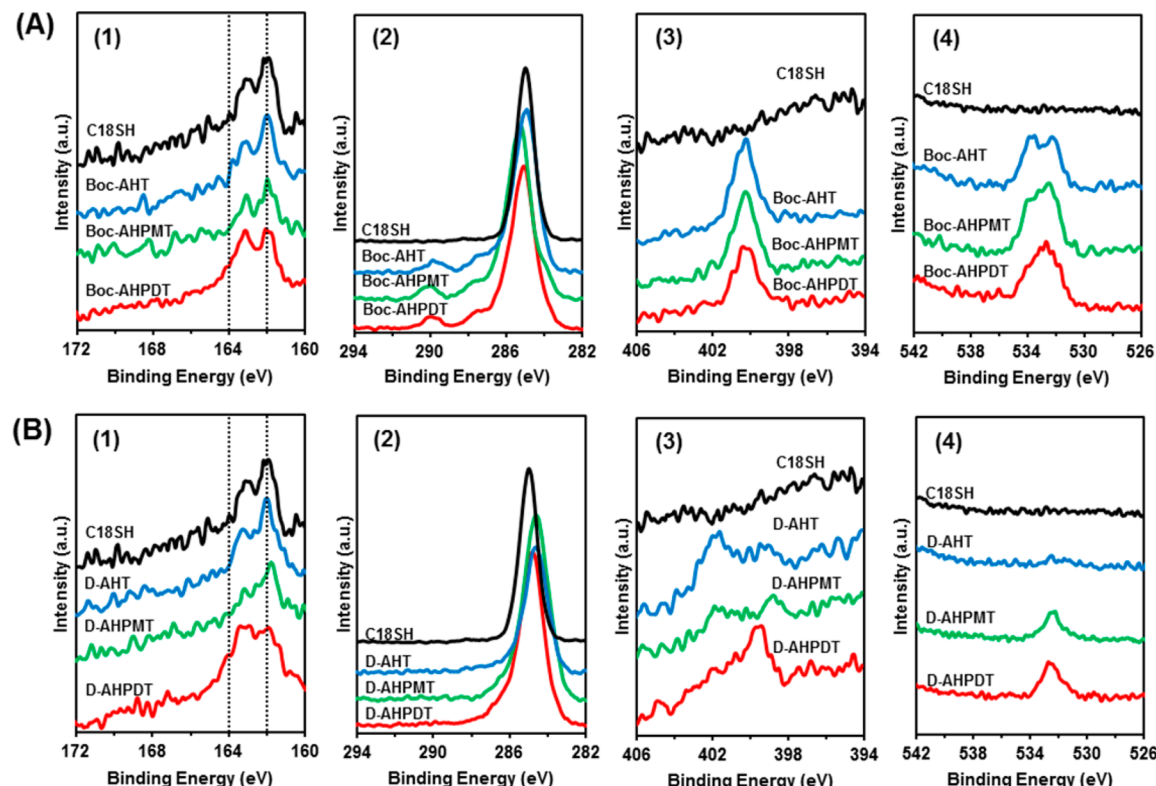


**Figure 5.** Comparison of the XPS spectra of the (1) S 2p, (2) C 1s, (3) N 1s, and (4) O 1s spectral regions of the films derived from Boc-AHT, Boc-AHPMT, and Boc-AHPDT (A) before and (B) after deprotection. The corresponding XPS spectra of a film generated from C18SH are shown for reference.

derived from the other adsorbates but also that the relative “crystallinity” of these films is Boc-AHPMT > Boc-AHPDT  $\approx$  Boc-AHT. These results are consistent with the data from the XPS C 1s spectra.

Overall, based on the analysis of the data for the ellipsometric thicknesses, XPS S 2p and C 1s spectral peak positions, and PM-IRRAS spectral peak positions, we conclude that the Boc-protected amine-terminated alkanethiols (Boc-AHT, Boc-AHPMT, and Boc-AHPDT) can readily form monolayers with  $\geq 85\%$  of bound thiolate on gold surfaces using ethanol as an adsorption medium. Furthermore, the relative packing density and conformational order of these films appears to be Boc-AHPMT > Boc-AHPDT  $\approx$  Boc-AHT. Owing to these results, we chose to more thoroughly investigate this set of SAMs to determine the impact of the deprotection process on these films. The resulting deprotected films are designated D-AHT, D-AHPMT, and D-AHPDT.

#### Characterization of Boc-Deprotected Amine-Terminated SAMs on Evaporated Gold Surfaces.

To activate the amino groups on the monolayer films generated from Boc-AHT, Boc-AHPMT, and Boc-AHPDT, we carried out the removal of the Boc protecting group using HCl solution (in dioxane, 4 M). Structural differences between the films before and after Boc deprotection were determined using ellipsometry, contact angle goniometry, XPS, and PM-IRRAS. The film thickness and interfacial wettability data are summarized in Table 2. The thickness of the Boc-AHPDT SAMs decreased by an average of 4 Å after deprotection. This change is consistent with the theoretical decrease in film thickness for the removal of the Boc protecting group ( $\sim 5$  Å). However, the reductions in film thickness of the Boc-AHT and Boc-AHPMT SAMs were 11 and 14 Å, respectively. The contact angles of water on the films were also evaluated before and after deprotection. The Boc-AHPDT films were completely wet after the removal of the Boc protecting group because of the high surface energy of the ammonium- or free amine-terminated surfaces.<sup>16,42</sup> However, the advancing contact angles ( $\theta_a$ ) for water on the Boc-AHT and Boc-AHPMT films after deprotection decreased

**Table 3. Comparison of the XPS-Derived Carbon-to-Gold (C/Au) and Sulfur-to-Gold (S/Au) Ratios to the Number of Adsorbate Carbons and Relative Packing Densities for the Films Generated from Boc-AHT, Boc-AHPMT, and Boc-AHPDT, before and after Deprotection**

	before deprotection (Boc-)			after deprotection (D-)			difference = after-before (difference/initial value × 100%)		
	AHT	AHPMT	AHPDT	AHT	AHPMT	AHPDT	AHT	AHPMT	AHPDT
C/Au	0.1018	0.1837	0.1575	0.0541	0.0847	0.1289	-0.0477 (-46%)	-0.0990 (-54%)	-0.0286 (-18%)
number of carbons in the adsorbate	21	28	29	16	23	24	-5 (-24%)	-5 (-18%)	-5 (-17%)
S/Au	0.0075	0.0088	0.0057 <sup>b</sup>	0.0061	0.0060	0.0057 <sup>b</sup>	-0.0014 (-18%)	-0.0028 (-32%)	~0 (~0%)
relative packing density <sup>a</sup>	82%	97%	63%	67%	66%	63%	-15% (-18%)	-31% (-32%)	~0% (~0%)

<sup>a</sup>The ratio of S/Au for the SAM formed from C18SH (0.0091) was used for estimating the packing densities, assuming that the C18SH film had a packing density of 100%. <sup>b</sup>To provide adequate comparison to the monodentate adsorbates, the S/Au ratio for Boc-AHPDT and D-AHPDT was divided by a factor of 2.

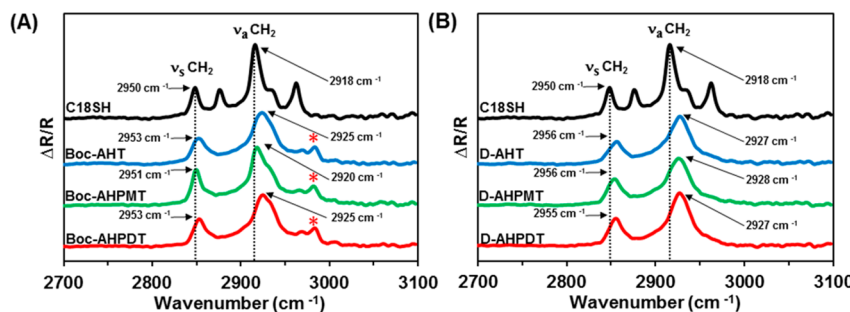


**Figure 6.** Comparison of the PM-IRRAS spectra for the C–H stretching region for the films generated from Boc-AHT, Boc-AHPMT, and Boc-AHPDT (A) before and (B) after deprotection. The corresponding PM-IRRAS spectrum of a film generated from C18SH is shown for reference.

24 and 27°, respectively, and the hysteresis ( $\Delta = \theta_a - \theta_r$ ) of both films increased,<sup>23</sup> yet neither of these surfaces was completely wet by water. The different behaviors of Boc-AHPDT and Boc-AHT/Boc-AHPMT upon deprotection will be discussed in a subsequent section.

The XPS spectra in Figure 5 provide evidence of the removal of the Boc protecting group. For the C 1s spectral region, peaks corresponding to the oxycarbonyl carbon (289.7 eV) and the *t*-butyl tertiary carbon (287.2 eV) disappeared after deprotection (Figure 5, plots A2 and B2).<sup>43</sup> And in the N 1s spectral region, the broad peak at 400.5 eV arising from the protecting group amide nitrogen (Figure 5, plot A3) disappears after deprotection, giving rise to two peaks at 401.9 eV for the protonated amino group and 400.2 eV for the free amino group (Figure 5, plot B3).<sup>43</sup> Finally, for the O 1s spectral region, the spectrum for D-AHT shows no peaks for oxygen, unlike that of Boc-AHT (Figure 5, plots A4 and B4); however, the O 1s spectra for D-AHPMT and D-AHPDT show diminished peaks for oxygen, as compared to the Boc-protected SAMs, associated with the oxygen in the backbone of the Boc-AHPMT and Boc-AHPDT adsorbates. Furthermore, the BEs of the methylene carbons and the carbons of the aromatic rings of the D-AHT, D-AHPMT, and D-AHPDT films in Figure 5 plot B2 are shifted to lower BEs than those of the Boc-AHT, Boc-AHPMT, and Boc-AHPDT films in Figure 5 plot A2 by 0.2, 0.6, and 0.4 eV, respectively. These results indicate that the packing densities of the films decreased upon removal of the Boc protecting group.

For a more quantitative evaluation of the changes to the Boc-protected amine-terminated films during the Boc deprotecting process, carbon-to-gold (C/Au) and sulfur-to-gold (S/Au) ratios obtained from the XPS spectra were prepared and analyzed (Table 3). These two ratios were calculated from the peak areas of the peaks associated with the C 1s, S 2p, and Au

4f BEs following methods described in previous reports.<sup>22,23,31</sup> The S/Au ratios can be used to calculate a relative packing density using a reference SAM with similar packing characteristics and film thickness. For our SAMs, we used a monolayer formed from C18SH as our reference system, assuming its packing density to be 100%.<sup>31</sup> Similarly, the C/Au ratios should provide a valuable perspective of these films in a comparison of the data before and after deprotection. Absent attenuation, the C/Au ratios of the Boc-AHT and Boc-AHPMT films would decrease by 24 and 18%, respectively, from each initial ratio after deprotection. However, the real decrements in C/Au ratios of the Boc-AHT and Boc-AHPMT films were 46 and 54%, respectively. Interestingly, the C/Au ratio of the Boc-AHPDT film decreased by only 18% upon deprotection. This experimental value came close to the value we calculated by assuming a rudimentary reduction of the C/Au ratio for the loss of the Boc protecting group. Furthermore, the relative packing density for the Boc-AHPDT film derived from the S/Au data remained the same before and after removal of the Boc protecting group. However, the relative packing densities for the Boc-AHT and Boc-AHPMT films decreased by 18 and 32%, respectively, from the initial values to those determined for the Boc-deprotected films. Overall, our results indicate that partial desorption occurs for the SAMs formed from the monodentate adsorbates (Boc-AHT and Boc-AHPMT) during the deprotection process, providing an explanation of the excessive reduction in film thickness for the Boc-AHT and Boc-AHPMT films after deprotection.

Two notable differences were detected in the PM-IRRAS spectra obtained before and after the Boc-deprotection procedure (Figure 6). First, the bands that corresponded to the Boc protecting groups (~2983 cm⁻¹) were not present in the spectra taken after deprotection, evidence that the termini of the chains no longer presented methyl groups at the SAM

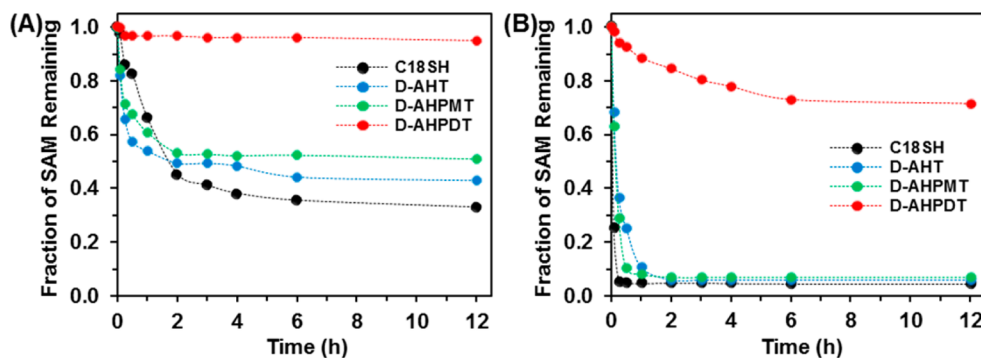


Figure 7. Solution-phase thermal desorption profiles of the indicated SAMs in decalin at (A) 70 and (B) 90 °C.

interface. Second, the band positions for  $\nu_{\text{as}}^{\text{CH}_2}$  for the D-AHT, D-AHPMT, and D-AHPDT films shifted to higher wave-numbers than those of the Boc-AHT, Boc-AHPMT, and Boc-AHPDT films by 2, 8, and 2  $\text{cm}^{-1}$ , respectively. These results indicate that the conformational order of these films decreased (i.e., the chains were not adopting predominantly trans-extended conformations), a change that can be rationalized by the presence of exposed amino groups bearing charges.

The aforementioned qualitative and quantitative analyses support the conclusion that the Boc-protected amine-terminated SAMs generated from Boc-AHPDT were readily converted to ammonium-/free amine-terminated SAMs that retained their surface coverage. In contrast, the Boc-AHT and Boc-AHPMT SAMs both lost adsorbate content during deprotection.

**Thermal Stability of Boc-Deprotected Amine-Terminated SAMs on Evaporated Gold Surfaces.** To evaluate the thermal stability of the SAMs formed from C18SH, D-AHT, D-AHPMT, and D-AHPDT on evaporated gold, we performed solution-phase thermal desorption experiments analogous to those detailed in a previous report.<sup>31</sup> In an initial set of experiments, we used ellipsometric thickness measurements to determine the average amount of adsorbate remaining after prolonged heating at 70 and 90 °C in a large excess of nonpolar solvent decalin (decahydronaphthalene). Figure 7 demonstrates the remarkable difference between the D-AHPDT films and the other films in our thermal stability test results. With a low level of applied heat (70 °C, Figure 7A), while more than 95% of the D-AHPDT adsorbates remained on the surface after 12 h, less than 50% of the adsorbates in the other SAMs remained under the same conditions. At a slightly higher temperature (90 °C, Figure 7B), while ~70% of the D-AHPDT adsorbates remained on the surface after 12 h, most of the adsorbates in the other SAMs detached from the gold surfaces after 1 h. These results can be interpreted to indicate that the SAMs derived from Boc-AHPDT are markedly more stable than the SAMs derived from Boc-AHT and Boc-AHPMT after deprotection. We can conclude from these results that the bidentate headgroup plays an important role in enhancing the thermal stability as well as the chemical stability for SAM adsorbates that are subjected to a deprotection procedure for their terminal moieties.

## CONCLUSIONS

Twelve adsorbates synthesized with either ammonium- or Boc-protected amine-termini and alkanethiol or alkanethioacetate headgroups were evaluated for their abilities to form well-ordered self-assembled monolayers on gold surfaces. An

analysis of these monolayers by ellipsometry, XPS, and PM-IRRAS revealed that the Boc-protected amine-terminated alkanethiols (Boc-AHT, Boc-AHPMT, and Boc-AHPDT) readily formed monolayers on evaporated gold surfaces, with ≥85% of their sulfur atoms forming bonds to the gold substrate. These custom-designed adsorbates ameliorate concerns associated with the use of amine-terminated SAMs generated from commercially available ammonium-terminated alkanethiols, such as the generation of oxidized sulfur species and carboxylated amine species and multilayer formation. Furthermore, the bidentate Boc-protected amine-terminated alkanethiol, Boc-AHPDT, showed remarkable chemical and thermal stability during the Boc-deprotecting process and the solution-phase thermal desorption tests, respectively.

## ASSOCIATED CONTENT

### Supporting Information

Detailed descriptions of the materials and synthesis procedures for preparing the ammonium- and Boc-protected amine-terminated alkanethiols/thioacetates, along with the instrumental procedures used to conduct this research. This material is available free of charge via the Internet at <http://pubs.acs.org>.

## AUTHOR INFORMATION

### Corresponding Author

\*E-mail: trlee@uh.edu.

### Notes

The authors declare no competing financial interest.

## ACKNOWLEDGMENTS

We thank the Robert A. Welch Foundation (grant no. E-1320) and the Texas Center for Superconductivity at the University of Houston for generous support.

## REFERENCES

- Opatkiewicz, J. P.; LeMieux, M. C.; Bao, Z. Influence of Electrostatic Interactions on Spin-Assembled Single-Walled Carbon Nanotube Networks on Amine-Functionalized Surfaces. *ACS Nano* **2010**, *4*, 1167–1177.
- Gupta, R. K.; Ying, G.; Srinivasan, M. P.; Lee, P. S. Covalent Assembly of Gold Nanoparticles: An Application toward Transistor Memory. *J. Phys. Chem. B* **2012**, *116*, 9784–9790.
- Yajima, S.; Furukawa, R. A.; Nagata, M.; Sakai, S.; Kondo, M.; Iida, K.; Dewa, T.; Nango, M. Two-dimensional patterning of bacterial light-harvesting 2 complexes on lipid-modified gold surface. *Appl. Phys. Lett.* **2012**, *100*, 233701.
- Bunimovich, Y. L.; Shin, Y. S.; Yeo, W.-S.; Amori, M.; Kwong, G.; Heath, J. R. Quantitative Real-Time Measurements of DNA

- Hybridization with Alkylated Nonoxidized Silicon Nanowires in Electrolyte Solution. *J. Am. Chem. Soc.* **2006**, *128*, 16323–16331.
- (5) Sen, T.; Bruce, I. J. Surface engineering of nanoparticles in suspension for particle based bio-sensing. *Sci. Rep.* **2012**, *2*, 1–6.
- (6) Brockman, J. R.; Frutos, A. G.; Corn, R. M. A Multistep Chemical Modification Procedure To Create DNA Arrays on Gold Surfaces for the Study of Protein-DNA Interactions with Surface Plasmon Resonance Imaging. *J. Am. Chem. Soc.* **1999**, *121*, 8044–8051.
- (7) Ho, M. Y.; D’Souza, N.; Migliorato, P. Electrochemical Aptamer-Based Sandwich Assays for the Detection of Explosives. *Anal. Chem.* **2012**, *84*, 4245–4247.
- (8) Wallace, A. F.; DeYoreo, J. J.; Dove, P. M. Kinetics of Silica Nucleation on Carboxyl- and Amine-Terminated Surfaces: Insights for Biomineralization. *J. Am. Chem. Soc.* **2009**, *131*, 5244–5250.
- (9) Vigderman, L.; Manna, P.; Zubarev, E. R. Quantitative Replacement of Cetyl Trimethylammonium Bromide by Cationic Thiol Ligands on the Surface of Gold Nanorods and Their Extremely Large Uptake by Cancer Cells. *Angew. Chem., Int. Ed.* **2012**, *51*, 636–641.
- (10) Wang, Q.; Moriyama, H. [60]-Fullerene and Single-Walled Carbon Nanotube-Based Ultrathin Films Stepwise Grafted onto a Self-Assembled Monolayer on ITO. *Langmuir* **2009**, *25*, 10834–10842.
- (11) Opatkiewicz, J. P.; LeMieux, M. C.; Liu, D.; Vosqueritchian, M.; Barman, S. N.; Elkins, C. M.; Hedrick, J.; Bao, Z. Using Nitrile Functional Groups to Replace Amines for Solution-Deposited Single-Walled Carbon Nanotube Network Films. *ACS Nano* **2012**, *6*, 4845–4853.
- (12) Blitz, J. P.; Shreedhara Murthy, R. S.; Leyden, D. E. Ammonia-Catalyzed Silylation Reactions of Cab-O-Sil with Methoxymethylsilanes. *J. Am. Chem. Soc.* **1987**, *109*, 7141–7145.
- (13) Love, J. C.; Estroff, L. A.; Kriebel, J. K.; Nuzzo, R. G.; Whitesides, G. M. Self-Assembled Monolayers of Thiolates on Metals as a Form of Nanotechnology. *Chem. Rev.* **2005**, *105*, 1103–1169.
- (14) Bang, G. S.; Park, J.; Lee, J.; Choi, H.-J.; Baek, H. Y.; Lee, H. Rose Bengal Dye on Thiol-Terminated Bilayer for Molecular Devices. *Langmuir* **2007**, *23*, 5195–5199.
- (15) Wang, H.; Chen, S.; Li, L.; Jiang, S. Improved Method for the Preparation of Carboxylic Acid and Amine Terminated Self-Assembled Monolayers of Alkanethiolates. *Langmuir* **2005**, *21*, 2633–2636.
- (16) Li, L.; Chen, S.; Jiang, S. Molecular-Scale Mixed Alkanethiol Monolayers of Different Terminal Groups on Au(111) by Low-Current Scanning Tunneling Microscopy. *Langmuir* **2003**, *19*, 3266–3271.
- (17) Baio, J. E.; Weidner, T.; Brison, J.; Graham, D. J.; Gamble, L. J.; Castner, D. G. Amine Terminated SAMs: Investigating Why Oxygen Is Present in These Films. *J. Electron Spectrosc. Relat. Phenom.* **2009**, *172*, 2–8.
- (18) Sprik, M.; Delamarche, E.; Michel, B.; Röthlisberger, U.; Klein, M. L.; Wolf, H.; Ringsdorf, H. Structure of Hydrophilic Self-Assembled Monolayers: A Combined Scanning Tunneling Microscopy and Computer Simulation Study. *Langmuir* **1994**, *10*, 4116–4130.
- (19) Fresco, Z. M.; Suez, I.; Backer, S. A.; Fréchet, J. M. J. AFM-Induced Amine Deprotection: Triggering Localized Bond Cleavage by Application of Tip/Substrate Voltage Bias for the Surface Self-Assembly of Nanosized Dendritic Objects. *J. Am. Chem. Soc.* **2004**, *126*, 8374–8375.
- (20) Unruh, D. A.; Mauldin, C.; Pastine, S. J.; Rolandi, M.; Fréchet, J. M. J. Bifunctional Patterning of Mixed Monolayer Surfaces Using Scanning Probe Lithography for Multiplexed Directed Assembly. *J. Am. Chem. Soc.* **2010**, *132*, 6890–6891.
- (21) Shestopalov, A. A.; Clark, R. L.; Toone, E. J. Catalytic Microcontact Printing on Chemically Functionalized H-Terminated Silicon. *Langmuir* **2010**, *26*, 1449–1451.
- (22) Shestopalov, A. A.; Clark, R. L.; Toone, E. J. Inkless Microcontact Printing on Self-Assembled Monolayers of Fmoc-Protected Aminothiols. *J. Am. Chem. Soc.* **2007**, *129*, 13818–13819.
- (23) Shestopalov, A. A.; Clark, R. L.; Toone, E. J. Inkless Microcontact Printing on SAMs of Boc- and TBS-Protected Thiols. *Nano Lett.* **2010**, *10*, 43–46.
- (24) Garg, N.; Lee, T. R. Self-Assembled Monolayers Based on Chelating Aromatic Dithiols on Gold. *Langmuir* **1998**, *14*, 3815–3819.
- (25) Shon, Y.-S.; Lee, S.; Colorado, R., Jr.; Perry, S. S.; Lee, T. R. Spiroalkanedithiol-Based SAMs Reveal Unique Insight into the Wettabilities and Frictional Properties of Organic Thin Films. *J. Am. Chem. Soc.* **2000**, *122*, 7556–7563.
- (26) Shon, Y.-S.; Lee, S.; Perry, S. S.; Lee, T. R. Adsorption of Unsymmetrical Spiroalkanedithiols onto Gold Affords Multi-Component Interfaces that Are Homogeneously Mixed at the Molecular Level. *J. Am. Chem. Soc.* **2000**, *122*, 1278–1281.
- (27) Park, J.-S.; Vo, A. N.; Barriet, D.; Shon, Y.-S.; Lee, T. R. Systematic Control of the Packing Density of Self-assembled Monolayers Using Bidentate and Tridentate Chelating Alkanethiols. *Langmuir* **2005**, *21*, 2902–2911.
- (28) Zhang, S.; Leem, G.; Srisombat, L.; Lee, T. R. Rationally Designed Ligands that Inhibit the Aggregation of Large Gold Nanoparticles in Solution. *J. Am. Chem. Soc.* **2008**, *130*, 113–120.
- (29) Srisombat, L.; Zhang, S.; Lee, T. R. Thermal Stability of Mono-, Bis-, and Tris-Chelating Alkanethiol Films Assembled on Gold Nanoparticles and Evaporated “Flat” Gold. *Langmuir* **2010**, *26*, 41–46.
- (30) Chinwangso, P.; Jamison, A. C.; Lee, T. R. Multidentate Adsorbates for Self-Assembled Monolayer Films. *Acc. Chem. Res.* **2011**, *44*, 511–519.
- (31) Lee, H. J.; Jamison, A. C.; Yuan, Y.; Li, C.-H.; Rittikulsittichai, S.; Rusakova, I.; Lee, T. R. Robust Carboxylic Acid-Terminated Organic Thin Films and Nanoparticle Protectants Generated from Bidentate Alkanethiols. *Langmuir* **2013**, *29*, 10432–10439.
- (32) Bruno, G.; Babudri, F.; Operamolla, A.; Bianco, G. V.; Losurdo, M.; Giangregorio, M. M.; Hassan Omar, O.; Mavelli, F.; Farinola, G. M.; Capezzuto, P.; Naso, F. Tailoring Density and Optical and Thermal Behavior of Gold Surfaces and Nanoparticles Exploiting Aromatic Dithiols. *Langmuir* **2010**, *26*, 8430–8440.
- (33) Bethencourt, M. I.; Srisombat, L.; Chinwangso, P.; Lee, T. R. SAMs on Gold Derived from the Direct Adsorption of Alkanethioacetates Are Inferior to Those Derived from the Direct Adsorption of Alkanethiols. *Langmuir* **2009**, *25*, 1265–1271.
- (34) Zhang, S.; Leem, G.; Lee, T. R. Monolayer-Protected Gold Nanoparticles Prepared Using Long-Chain Alkanethioacetates. *Langmuir* **2009**, *25*, 13855–13860.
- (35) Castner, D. G.; Hinds, K.; Grainger, D. W. X-ray Photoelectron Spectroscopy Sulfur 2p Study of Organic Thiol and Disulfide Binding Interactions with Gold Surfaces. *Langmuir* **1996**, *12*, 5083–5086.
- (36) Singhana, B.; Rittikulsittichai, S.; Lee, T. R. Tridentate Adsorbates with Cyclohexyl endgroups Assembled on Gold. *Langmuir* **2013**, *29*, 561–569.
- (37) Ishida, T.; Hara, M.; Kojima, I.; Tsuneda, S.; Nishida, N.; Sasabe, H.; Knoll, W. High Resolution X-ray Photoelectron Spectroscopy Measurements of Octadecanethiol Self-Assembled Monolayers on Au(111). *Langmuir* **1998**, *14*, 2092–2096.
- (38) Wühn, M.; Weckesser, J.; Wöll, Ch. Bonding and Orientational Ordering of Long-Chain Carboxylic Acids on Cu(111): Investigations Using X-ray Absorption Spectroscopy. *Langmuir* **2001**, *17*, 7605–7612.
- (39) Nuzzo, R. G.; Dubois, L. H.; Allara, D. L. Fundamental Studies of Microscopic Wetting on Organic Surfaces. 1. Formation and Structural Characterization of a Self-Consistent Series of Polyfunctional Organic Monolayers. *J. Am. Chem. Soc.* **1990**, *112*, 558–569.
- (40) Bensebaa, F.; Voicu, R.; Huron, L.; Ellis, T. H.; Kruus, E. Kinetics of Formation of Long-Chain n-Alkanethiolate Monolayers on Polycrystalline Gold. *Langmuir* **1997**, *13*, 5335–5340.
- (41) Porter, M. D.; Bright, T. B.; Allara, D. L.; Chidsey, C. E. D. Spontaneously Organized Molecular Assemblies. 4. Structural Characterization of n-Alkyl Thiol Monolayers on Gold by Optical Ellipsometry, Infrared Spectroscopy, and Electrochemistry. *J. Am. Chem. Soc.* **1987**, *109*, 3559–3568.
- (42) Bain, C. D.; Troughton, E. B.; Tao, Y. T.; Evall, J.; Whitesides, G. M.; Nuzzo, R. G. Formation of monolayer films by the spontaneous assembly of organic thiols from solution onto gold. *J. Am. Chem. Soc.* **1989**, *111*, 321–325.

(43) Strother, T.; Hamers, R. J.; Smith, L. M. Covalent Attachment of Oligodeoxyribonucleotides to amine-modified Si (001) Surfaces. *Nucleic Acids Res.* **2000**, *28*, 3535–3541.